INTERNATIONAL SOCIETY FOR SOIL MECHANICS AND GEOTECHNICAL ENGINEERING

SIMSG   ISSMGE

Influence of Kinematic SSI on Foundation Input Motions for Pile-Supported Bridges

B. J. Turner[1], S. J. Brandenberg[2], J. P. Stewart[3]

ABSTRACT

The seismic analysis of bridge structures is often performed using the substructure method in which the foundation is replaced by an equivalent "spring" representing foundation impedance. Ground motions from seismic hazard analyses correspond to a free-field condition, and therefore should be modified to account for kinematic soil-structure interaction effects before being used as input to the springs. This paper presents closed-form analytical solutions for the response of an elastic pile subjected to harmonic seismic excitation in uniform elastic soil. We use these solutions to compute transfer functions relating foundation input motion to free-field ground motion and use the results to verify predictions from a beam-on-Winkler-foundation numerical model. The two approaches show good agreement, indicating that the numerical modeling method is appropriate for investigating more complex effects such as soil and pile nonlinearity. Ground motion deamplification due to kinematic SSI is demonstrated to be significant for stiff foundations in soft ground conditions. Numerical simulations using recorded ground motions demonstrates that transfer functions can be computed only from frequency bands for which the motions contain adequate energy.

Introduction

Seismic design of bridges and other structures supported on bored or driven piles often utilize a substructure method in which the foundation elements are not explicitly modeled, but rather are replaced by "springs" representing the foundation impedance. The ground motion appropriate for input to the free-end of the springs (i.e., the foundation input motion, FIM) differs from the free-field motion (FFM) due to kinematic soil-structure interaction (SSI). Ground motions from a seismic hazard analysis represent shaking in the free field. For example, pseudo-spectral accelerations (*PSa*) on seismic hazard maps and site amplification factors used in building codes and seismic design guidelines (e.g., ASCE-7, 2010) do not include the influence of SSI. Similarly, the PEER ground motions database (Ancheta et al., 2014), a commonly used source for accelerograms used in response history analyses, excludes records influenced by SSI.

Past studies of kinematic SSI for pile foundations used analytical and numerical solutions. Flores-Berrones and Whitman (1982), Fan et al. (1991), and Nikolaou et al. (2001) quantify the kinematic response of vertical piles and pile groups for vertically propagating shear waves in elastic soil. Similar solutions for inclined waves have been presented by Barghouthi (1984), Mamoon and Banerjee (1990), and Kaynia and Novak (1992). Taking the FIM as the pile head motion, the ratio FIM/FFM can be expressed as a frequency-dependent transfer function. These

---
[1]Ph.D. Candidate, Dept. Civil & Environ. Eng., University of California, Los Angeles, USA, bjturner@ucla.edu
[2]Assoc. Professor and Vice Chair, Dept. Civil & Environ. Eng., UCLA, USA, sjbrandenberg@ucla.edu
[3]Professor and Chair, Dept. Civil & Environ. Eng., UCLA, USA, jstewart@seas.ucla.edu

studies have found that at low frequencies, the transfer function ordinate (H_u) is approximately unity, indicating that the soil and pile move in unison. At higher frequencies, a relatively stiff pile will not conform to the short-wavelength ground motion, so H_u decreases. Whether or not H_u descends below unity within the frequency range of engineering interest for a bridge depends on factors such as the relative stiffness contrast between the pile and soil, the length of the pile, and whether or not restraint against rotation is provided at the pile head. Examinations of data from pile-supported buildings, where base-slab averaging (and in some cases, embedment) effects act in combination with the kinematics of soil-pile interaction to produce observations of H_u have suggested both an apparently negligible effect of piles (Kim and Stewart 2003) and potentially significant effects (Givens et al. 2012). These discrepancies have yet to be satisfactorily resolved.

A comprehensive study of kinematic SSI effects including nonlinear site response, soil and pile nonlinearity, frequency content, group interaction, and ground motion incoherence is currently underway by the authors. The analyses utilize a beam-on-nonlinear-Winkler-foundation (BNWF) model attached through *p-y* springs to soil nodes. The soil nodes are excited by displacement records which represent the free-field ground response at each depth along the length of the pile, and the model is analyzed using the finite element program *OpenSees* (Mazzoni et al. 2007). No mass is assigned in the model; the absence of inertial forces allows kinematic soil-structure interaction (KSSI) effects to be isolated.

This paper focuses on validation of the BNWF modeling approach for a vertical elastic pile in uniform, undamped elastic soil using closed-form solutions. We derive a closed-form analytical solution for the transfer function and subsequently compare it to the results of a linear-elastic Winkler foundation model analyzed in *OpenSees*. Input ground motions include harmonic sweep functions that are rich in frequency content across a wide bandwidth and recorded ground motions having variable mean periods. Depth-dependent ground motions are computed from the surface motions based on linear elastic wave propagation theory. Comparisons between the analytical and numerical solutions are presented in this paper. Nonlinear soil and pile effects, ground motion incoherence, and comparison to field data are reserved for future studies.

Analytical Solution

Derivation of the closed-form solution for a vertical elastic pile in elastic soil begins with the following fourth-order differential equation for a laterally-loaded pile in the absence of free-field ground motion (after Hetenyi 1946):

$$\frac{d^4 u_p}{dz^4} EI + \frac{d^2 u_p}{dz^2} P - k_y u_p = 0 \tag{1}$$

in which u_p is horizontal pile displacement, z is depth measured downwards from the pile head, EI is the pile flexural rigidity, P is axial load, and k_y is the soil-pile interaction stiffness intensity, all defined in a consistent set of units. For our purposes, axial load is taken as zero and the displacement term is replaced with the relative displacement between the pile and free field soil undergoing horizontal displacement consistent with harmonic seismic excitation by vertically propagating shear waves:

$$\frac{d^4 u_p}{dz^4} EI + k_y [u_p - u_{g0} \cos(kz)] = 0 \tag{2}$$

where u_{g0} is the ground displacement at the surface due to the harmonic seismic excitation and k is the wave number defined as the ratio of excitation angular frequency (ω) to soil shear wave velocity (V_s). The solution to Equation 2 in terms of pile horizontal displacement at depth z as a function of the previously defined variables is:

$$u_p(z) = e^{Rz} \cos(Rz) \chi_1 + e^{Rz} \sin(Rz) \chi_2 + e^{-Rz} \cos(-Rz) \chi_3 + e^{-Rz} \sin(-Rz) \chi_4 + \frac{k_y u_{g0}}{EI \cdot k^4 + k_y} \cos(kz) \tag{3}$$

where χ_1 through χ_4 are constants and R is a dimensionless variable combining terms as follows:

$$R = \sqrt[4]{\frac{k_y}{4EI}} \tag{4}$$

Successive derivatives of Equation 3 provide expressions for slope, curvature, moment, shear, and soil reaction. The expressions for slope (S), moment (M), and shear (V) are:

$$S(z) = \frac{du_p}{dz} = R\left[e^{Rz}\left(A\chi_1 + B\chi_2\right) - e^{-Rz}\left(B\chi_3 + A\chi_4\right)\right] - k \cdot C \sin(kz) \tag{5}$$

$$M(z) = \frac{d^2 u_p}{dz^2} EI = EI\left(2R^2\left\{e^{Rz}\left[-\sin(Rz)\chi_1 + \cos(Rz)\chi_2\right] + e^{-Rz}\left[\sin(Rz)\chi_3 + \cos(Rz)\chi_4\right]\right\} - k^2 C \cos(kz)\right) \tag{6}$$

$$V(z) = \frac{d^3 u_p}{dz^3} EI = EI\left(2R^3\left[e^{Rz}\left(-B\chi_1 + A\chi_2\right) + e^{-Rz}\left(A\chi_3 - B\chi_4\right)\right] + k^3 C \sin(kz)\right) \tag{7}$$

The following substitutions were used to abbreviate Equations 5, 6 and 7:

$$A = \cos(Rz) - \sin(Rz) \ ; \quad B = \cos(Rz) + \sin(Rz) \ ; \quad C = \frac{k_y u_{g0}}{EI \cdot k^4 + k_y} \tag{8}$$

To solve for the constants χ_1 through χ_4, a set of four permissible boundary conditions must be imposed. Typically the boundary conditions are prescribed at the pile head and tip since these can be determined on the basis of details such as embedment into a pile cap or a stiff bearing stratum. For example, in the absence of superstructure force or moment demands (required for a KSSI analysis) the boundary conditions for a fixed-head, free-tip pile of length L are:

$$V(z=0) = 0 \ ; \quad S(z=0) = 0 \ ; \quad V(z=L) = 0 \ ; \quad M(z=L) = 0 \tag{9}$$

The appropriate expressions for displacement, slope, shear, and moment provided by Equations 3, 5, 6, and 7 can be equated to the specified boundary conditions at the pile head and tip to form a system of four equations which can be solved to evaluate χ_1 through χ_4.

Pile head displacement is evaluated using Equation 3 at depth $z = 0$. To produce an analytical transfer function, the pile head displacement normalized by the amplitude of the harmonic ground motion, u_{g0}, is evaluated as a function of frequency.

Numerical Solution

The numerical modeling approach consists of an elastic pile discretized into 0.1-m segments and attached to linear-elastic soil springs at each node. We modeled the pile and soil using elastic beam-column and elastic zero-length uniaxial materials, respectively, in *OpenSees*.

We considered two categories of input excitation, sine-sweep motions consisting of uniform-displacement amplitude broadband frequency content from 0.1 to 50 Hz, and recorded ground motions with variable bandwidth. The free-field input motions were specified at the ground surface and motions at the depth of each soil spring were computed by convolving the input motion (Equation 10) based on assumptions of uniform, elastic undamped soil and zero shear strain at the ground surface (after Kramer 1996):

$$u_g(z) = u_{g0} \cdot \cos(k \cdot z) \tag{10}$$

Note that this transfer function is distinct from the transfer functions relating pile head motion to u_{g0} and is only used to compute free-field soil displacement at each depth increment. By specifying the input motion at the ground surface rather than the base of the soil profile, the problem of infinite amplification at resonant site frequencies is avoided. The amplitude of the input excitation does not affect the computed transfer functions since the model is linear-elastic.

Soil and pile properties for the numerical analyses match the properties used in the analytical solution so that a direct comparison of the computed transfer functions can be made. We defined the soil-pile interaction stiffness (k_y) at depth z as (Gazetas and Dobry 1984):

$$k_y = 1.69 E_s \left(\frac{E_p}{E_s(z)} \right)^{-0.137} \quad ; \quad E_s(z) = 2\rho V_s^2 (1+v) \tag{11}$$

where E_p is the pile elastic modulus, taken as 2.7E7 kPa for reinforced concrete, and E_s is depth-dependent elastic soil modulus computed from V_s based on classical elasticity theory with assumed soil density ρ=1.6 Mg/m^3 and Poisson's ratio v=0.3. The uniaxial spring stiffness is defined as k_y divided by the tributary length of the pile element to which it is attached. The soil springs connected to the pile head and tip are assigned a tributary length equal to half of the pile segment discretization length.
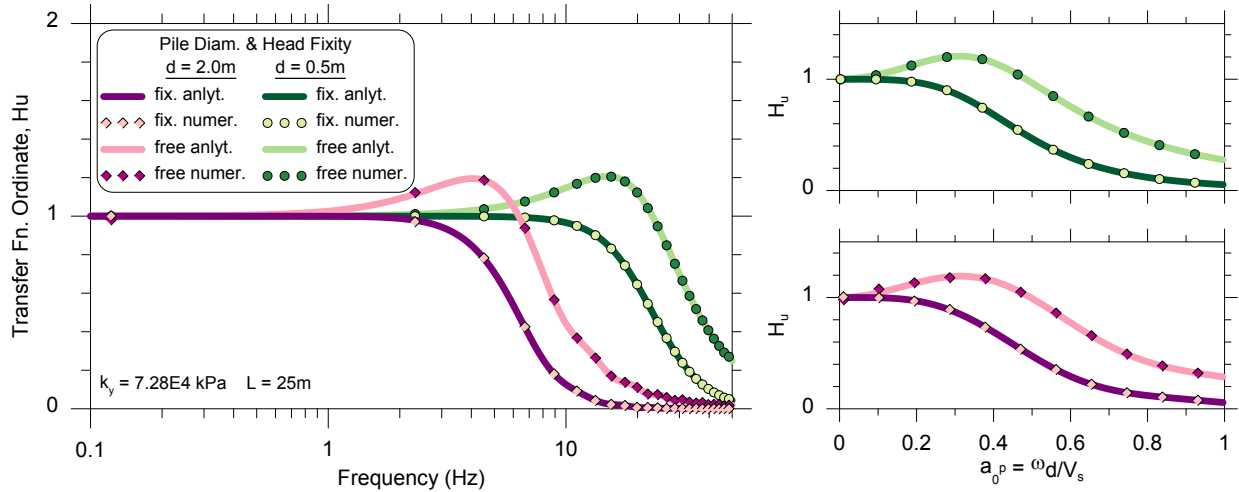
Figure 1: Analytical and numerical solution transfer functions for sine-sweep input motion.
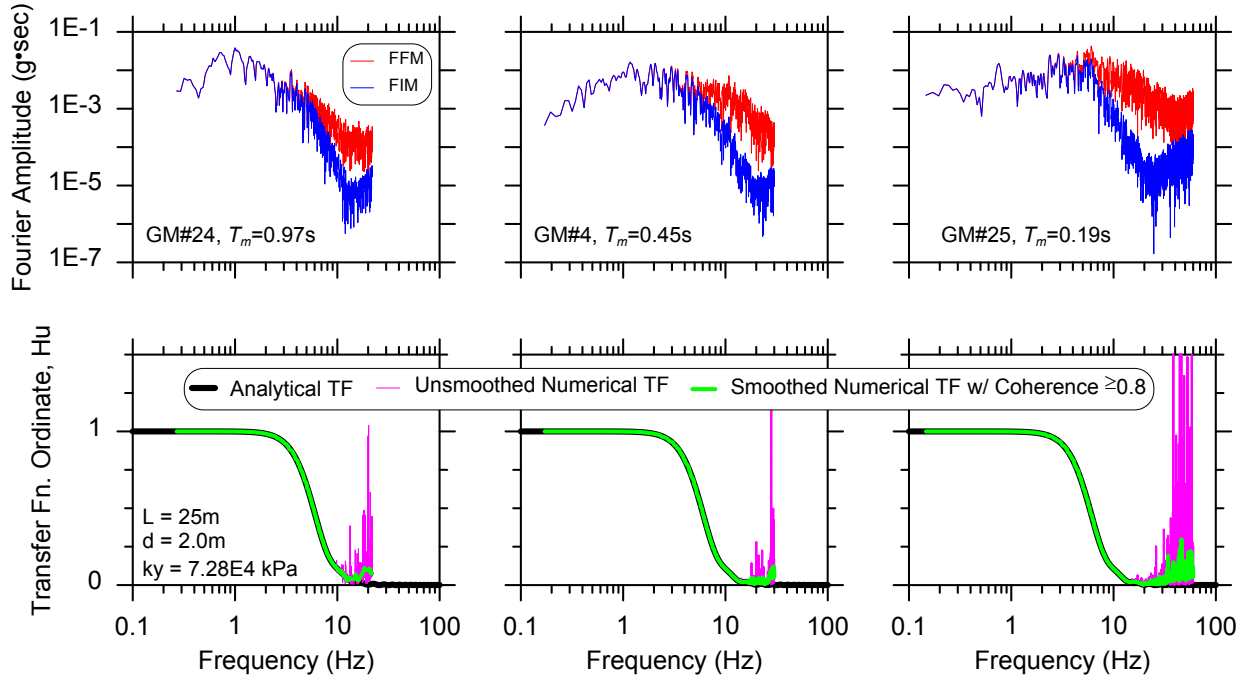

Figure 2: Fourier amplitude spectra for free-field and foundation-input motions (top) and corresponding transfer functions (bottom).

Results

Transfer functions for the analytical solution are compared to the numerical solution results for a sine-sweep input motion in Figure 1 and for recorded earthquake ground motions in Figure 2. Two sizes of circular concrete piles are considered for the analytical solutions, 0.5-m and 2.0-m diameter (d), for a site with V_s=150m/s. Both fixed-head and free-head restraint conditions are considered. For the numerical solution, only the 2.0-m diameter fixed-head pile is considered.

The sine-sweep input motion transfer functions show near-perfect agreement with the analytical solution over the entire frequency range considered for both pile sizes. Free-head piles are seen to exhibit amplification of the input motion ($H_u > 1$) of about 20% at a dimensionless frequency (a_0^p) of about 0.3. This contradicts the frequently held notion that the FIM is always less than the FFM and thus can always safely be ignored for a "conservative" design. The right side of Figure 1 shows that solutions for different pile sizes converge when frequency is normalized to a_0^p

For the comparisons using real earthquake ground motions as input, we characterized the frequency content of the motions based on mean period, T_m (Rathje et al. 1998). The inverse of T_m, which is the mean frequency (although Rathje et al. do not use this terminology), represents the motion's central frequency (approximate centroid of Fourier amplitude spectrum). We use ground motions from a set of 40 records with broad frequency content and statistical variability compiled by Baker et al. (2011). For the current comparison, we selected from the set of 40 the motions with the minimum, median, and maximum T_m as shown in Table 1.

Table 1: Ground motions for numerical analyses; numbering follows Baker et al. (2011)

Motion #	Earthquake	Recording Station	M	T_m (s)	PGA (s)
25	1989 Loma Prieta	UCSC	6.9	0.19	0.34
4	1994 Northridge	LA – Wonderland Ave.	6.7	0.45	0.13
24	1989 Loma Prieta	Golden Gate Bridge	6.9	0.97	0.16

Figure 2(a) shows acceleration Fourier amplitude spectra (FAS) for the pile head motion (FIM) and ground surface motion (FFM) for each of the three input earthquakes we considered. Note that each ground motion FAS is only plotted over the useable frequency range of the ground motion, which depends on the processing applied to the original recording (Ancheta et al. 2014). The ratio of the displacement FAS is the unsmoothed transfer function shown in Figure 2(b).

Transfer functions generated using the earthquake input motions highlight an important issue in the proposed numerical modeling approach. Because the motions we considered have near-zero Fourier amplitude in the frequency range greater than about 10 Hz (notice for example in Figure 2(a) that the Fourier amplitude at a frequency of 20 Hz is about 3 to 4 orders of magnitude less than at 1 Hz), small errors in the computed pile displacements at these higher frequencies result in large amplification, with H_u approaching 2.0 in some cases. Mathematically, this arises because the very small pile head motion is being divided by an even smaller ground displacement that is essentially zero. The pile head motions are in fact so small that they may be attributable to numerical oscillations in the finite element solution.

Kim and Stewart (2003) address this issue by utilizing an alternative transfer function definition:

$$H_u(\omega) = \sqrt{S_{xx}(\omega)/S_{yy}(\omega)} \tag{12}$$

where S_{xx} and S_{yy} are the smoothed auto power spectral density functions of the FIM and FFM, respectively. The smoothing operation is accomplished by replacing each ordinate of the unsmoothed power spectrum with a weighted average value of the unsmoothed ordinates over a

frequency band centered on the point of interest. We used an 11-point Hamming window to perform the smoothing in the frequency domain. In addition, we considered the coherence between the FFM and FIM as a means of discerning which transfer function ordinates represent meaningful frequency content in the ground motion. Details of the smoothing operation and coherence computation are omitted for brevity and can be found in Kim and Stewart (2003) and Mikami et al. (2008). Figure 2(b) shows the smoothed transfer functions plotted only at ordinates with coherence greater than or equal to 0.8, which eliminates much of the noise seen in the unsmoothed transfer functions and provides a closer match to the analytical transfer functions.

Finally, we computed ratio-of-response-spectra (RRS) for the three ground motions, defined as the ratio of pseudo response spectrum ordinates (PSa) for a damped single-degree-of-freedom (SDOF) oscillator subjected in turn to the FIM and FFM (Figure 3). Since the high frequency portion of a response spectrum is controlled by the amplitude of the largest spike in the ground motion rather than the high frequency content of the ground motion, the SDOF oscillator effectively acts like a high frequency (low pass) filter (NIST 2012). As a result, the short period region of the RRS does not contain the high frequency spikes seen in the unsmoothed numerical transfer functions. Figure 3 clearly demonstrates that the RRS depends strongly on the frequency content and resulting spectral shape of the free-field motion, since motions with a higher mean frequency will be more effectively attenuated by the pile.
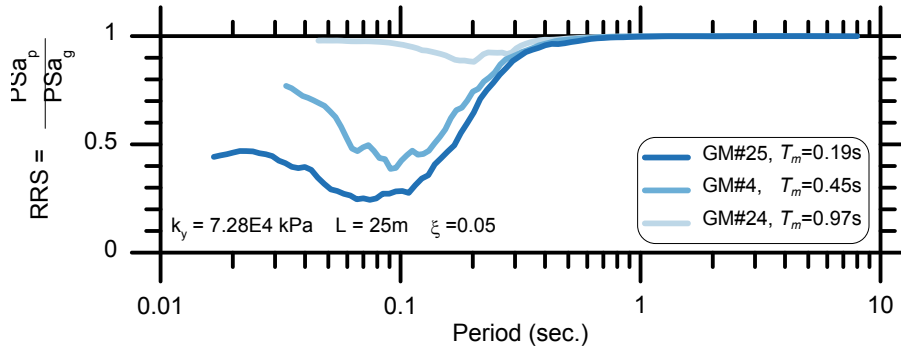

Figure 3: Ratio-of-Response-Spectra for 2.0-m diameter fixed-head pile.

Conclusion

We have presented closed-form analytical solutions for the response of a vertical pile subjected to harmonic excitation from vertically propagating shear waves. The results are expressed as transfer functions between the pile head motion and free-field motion. We compared the analytical results to transfer functions generated using a linear-elastic beam-on-Winkler-foundation model and demonstrated that foundation input motions computed using the numerical approach are in excellent agreement with the analytical solution for a sine-sweep input motion that is rich in frequency content. For the recorded motions, we showed that the numerical transfer functions are in good agreement with the analytical solutions over frequency bands with high coherence between the ground motion and the foundation motion.

We find the free-field ground motion amplitude to be reduced substantially for frequencies above about 2 to 20 Hz ($a_0{}^p$=0.2-0.3). We expect that the introduction of soil nonlinearity to the

numerical model will shift the affected frequencies further into the range of engineering interest for large bridges (roughly 0.2 to 2 Hz).

Acknowledgments

References

American Soc. of Civil Engineers. *ASCE/SEI 7-10, Min. Design Loads for Bldg. and Other Struc*. Reston, VA, 2010

Ancheta TD, Darragh RB, Stewart JP, Seyhan E., Silva WJ, Chiou BSJ, Woodell KE, Graves RW, Kottke AR, Boore DM, Kishida T., and Donahue JL. *NGA-West2 Database*, Earthq. Spectra, 2014; **30**(3), 980-1005.

Baker JW, Lin T., Shahi SK, and Jayaram N. *New Ground Motion Selection Procedures and Selected Motions for the PEER Transportation Research Program*. PEER Technical Report 2011/03, 2011.

Barghouthi AF. *Pile Response to Seismic Waves*. PhD Thesis, Univ. of Wisconsin, Madison, 1984.

Fan K., Gazetas G., Kaynia A., and Kausal E. *Kinematic Seismic Response of Single Piles and Pile Groups*. J. Geotech. and Geoenviron. Eng. 1991; **117**(12), 1860-1879.

Flores-Berrones R., and Whitman RV. *Seismic Response of End-Bearing Piles*. J. Geot. Eng. 1982; **108**(4), 554-569.

Gazetas G., and Dobry R. *Horizontal Response of Piles in Layered Soils*. J. Geotech. Eng. 1984; **110**(1), 20-40.

Givens MJ, Mikami A, Kashima T, and Stewart JP. *Kinematic Soil-Structure Interaction Effects from Building and Free-Field Seismic Arrays in Japan*. Proc. 9th International Conf. on Urban Earthquake Engin./4th Asia Conf. on Earthquake Eng., 2012, Tokyo Institute of Technology, Tokyo, Japan.

Hetenyi M. *Beams on Elastic Foundation*, University of Michigan Press, Ann Arbor, Michigan, 1946.

Kaynia AM, and Novak M. *Response of Pile Foundations to Rayleigh Waves and to Obliquely Incident Body Waves*. Earthq. Eng. and Struct. Dyn. 1992; **21**(4), 303-318.

Kim S., and Stewart JP. *Kinematic soil-structure interaction from strong motion recordings*. J. Geotech. and Geoenviron. Eng. 2003; **129**(4), 323-335.

Kramer S. *Geotechnical Earthquake Engineering*. Prentice-Hall, Upper Saddle River, NJ, 1996.

Mamoon SM, and Banerjee PK. *Response of Piles and Pile Groups to Traveling SH-waves*. Earthq. Eng. and Struct. Dyn. 1990; **19**(4), 597-610.

Mazzoni S., McKenna FT, Scott MH, and Fenves GL. *OpenSees Command Language Manual*, Pacific Earthquake Engineering Research (PEER) Center, University of California, Berkeley, CA, 2006.

Mikami A., Stewart JP, and Kamiyama M. Effects of Time Series Analysis Protocols on Transfer Functions Calculated from Earthquake Accelerograms. Soil Dyn. and Earthq. Eng. 2008; **28**(9), 695-706.

Nikolaou S., Mylonakis G., and Tazoh T. *Kinematic Pile Bending During Earthquakes; Analysis and Field Measurements*. Géotechnique 2001; **51**(5), 425-440.

National Institute of Standards and Technology (NIST). *Soil-Structure Interaction for Building Structures*. 2012.

Rathje E., Abrahamson N., and Bray J. *Simplified Frequency Content Estimates of Earthquake Ground Motions*. J. and Geotech. Geoenviron. Eng. 1998; **124**(2), 150–159.